Project of a rear-end collision safety device

Douglas Dias
FEI University

Hemanoelly Silva
FEI University

Igor Nogueira
FEI University

Leonardo Bertanha
FEI University

Leonardo Perrotta
FEI University

Lucas Claudio
FEI University

ABSTRACT

According to historical data from the Federal Highway Police (PRF) [1], a total of 32,564 two-vehicle collisions were recorded on Brazilian highways in 2022. Of these, 37% equivalent to 12,082 accidents were identified as rear-end collisions, resulting in 13,868 victims. These types of accidents are particularly concerning due to the heightened risk of severe injuries, especially for third-row occupants in larger vehicles such as SUVs and minivans.

This study proposes a solution to reduce intrusion in rear-end collisions involving passenger vehicles designed to accommodate seven or more occupants. Given the widespread use of such vehicles by families and for commercial transportation, ensuring the safety of third-row passengers is a critical concern. A structural reinforcement strategy was developed and evaluated using advanced engineering tools to mitigate impact forces in rear-end crash scenarios. The results demonstrated a substantial reduction in intrusion of 40% in low-speed impacts and 16% in high-speed impacts, then enhancing occupant protection and lowering the risk of injury.

Beyond safety benefits, the proposed solution is technically feasible and integrates seamlessly with existing vehicle structures, requiring minimal modifications to the original design.

INTRODUCTION

Global mobility is experiencing continuous growth. The demand for efficient, practical, and safe transportation has become increasingly critical, especially in light of the rapid expansion of metropolitan areas worldwide. Vehicles in the SUV and MPV segments offer advantages by prioritizing family travel and versatility. Certain models are homologated to transport seven or more occupants, thereby reducing the number of vehicles required and, consequently, minimizing travel time when compared to vans, trailers, or buses.

Additionally, according to data from the Ministry of Tourism (MTur) survey, 74% of Brazilians who took leisure trips up to March 2024 traveled either by private vehicle or bus. This underscores the growing importance of car use for families and, consequently, the increasing tendency to utilize seven-seater vehicles for such journeys.

It is also relevant to note that the additional seats located in the third row are predominantly occupied by children, due to their smaller stature, the dimensions of the seats, and the novelty factor. This significantly heightens the relevance of the topic addressed in this study, as the safety of child passengers is at increased risk in rear-end collisions involving this category of vehicles.

An analysis of the most frequent accident types on Brazilian highways, based on data collected by the Federal Highway Police (PRF) and illustrated in Figure 1, clearly highlights the high incidence of injuries and fatalities resulting from rear-end collisions—with approximately 578 deaths recorded in 2022 alone.

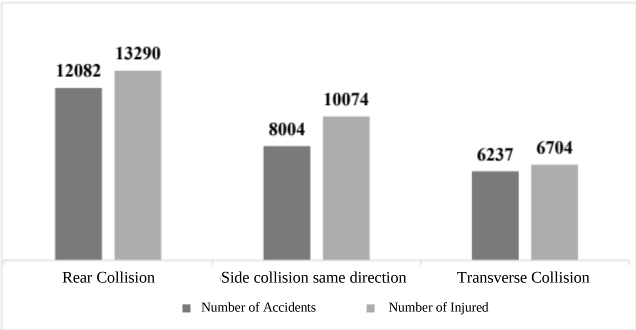

Figure 1: Number of Accidents and their types of Collision in 2022.
Source: Authorship based on data from the PRF Yearbook Report, 2022.

When it comes to vehicle safety, the standards for mass-produced vehicles require an extensive series of tests to meet the various existing standards. Currently, automakers rely on European standards (ECE) or North American standards (FMVSS) to produce their vehicles.

With the advent of globalization, many local regulations are now based on the guidelines established by the international bodies to regulate vehicles traded globally. As illustrated in Figure 2, increasing the number of seating rows reduces the distance between the rear of the vehicle and the last-row occupant. Using a premium seven-seater SUV as an example, this distance in a five-occupant configuration measures approximately 1,397 mm, as shown in Figure 2.

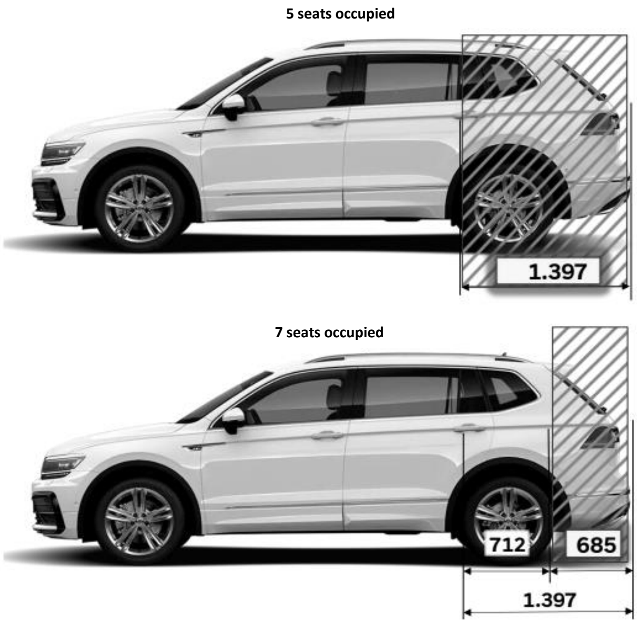

Figure 2: Comparison of available space for intrusion
Source: DIMARVE [2]

In the context of standards related to rear-impact collisions, although several regulations are applicable, as of the date of this study's development and completion, no specific standard has been identified that comprehensively addresses body intrusion in rear-end collisions, particularly in vehicles equipped with third-row seating.

Given this gap, the study was guided by two key standards, as illustrated in Figure 3, both of which aim to protect the fuel tank area during rear-end impacts: Brazil's CONTRAN Resolution No. 721 [3], which aligns with the ECE-R32 regulation, and FMVSS 301, which differs in the test execution methodology.

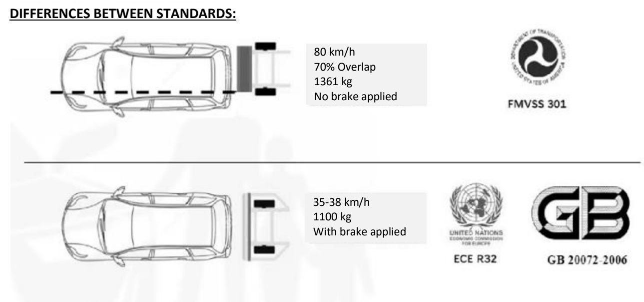

Figure 3: Differences between FMVSS 301, ECE-R32/GB20072-2006 Standards
Source: Authorship based on data from ENRST GRUPPE

The differences between the FMVSS 301 and ECE-R32 standards lie primarily in test execution parameters. Under ECE-R32, the mobile barrier weighs 1,100 kg and impacts 100% of the rear area of a stationary vehicle (with the parking brake applied) at a speed of around 35 to 38 km/h. In contrast, FMVSS 301 employs a slightly heavier barrier weighing 1,361 kg, which impacts 70% of the vehicle's rear without the parking brake applied, but at a significantly higher speed of 80 km/h.

Based on these standards and through the application of engineering tools such as Benchmarking, P-Diagram, FMEA and a decision matrix, the project was initiated with the goal of enhancing protection for third-row occupants.

To this end, a comparative analysis was conducted among various structural solutions already established in the automotive market. The objective was to identify the concept with the highest potential for integration into the project, based on criteria such as ease of implementation, production feasibility, and safety performance.

The selection of the most appropriate concept was carried out using a decision matrix, which resulted in the choice of a system based on changing the material of key structural components: the D-pillar, the side panel, the rear D-crossmember, and the closing crossmember. The original 260 BH steel was replaced by SAE-AISI 81B45, while preserving the existing geometries.

To complement this material upgrade, an energy-absorbing plate was added, inspired by the attenuating systems typically found in the front-end structures of vehicles. This solution includes mounting brackets designed to deform in a controlled manner during impact, thereby maximizing energy absorption and minimizing structural intrusion.

The rear impact absorption system consists of two lateral supports aligned with the vehicle's rear longitudinal members, manufactured from 5059-H321 alloy, and an attenuation plate made from EM-MC 21110 material. Figures 4, 5, and 6 illustrate the components of the absorption system.

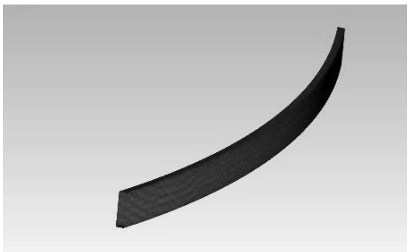

Figure 4: Rear-end impact beam
Source: Authorship using simulation software.

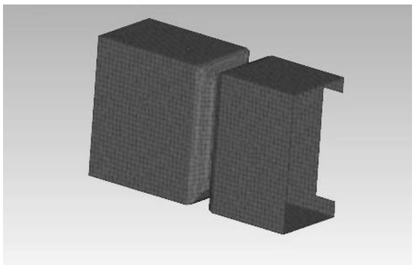

Figure 5: Rear-end impact beam support
Source: Authorship using simulation software.

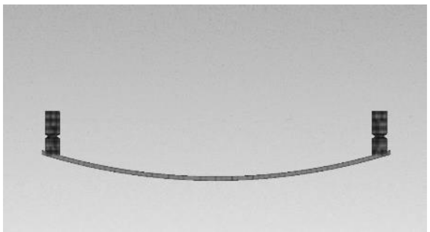

Figure 6: Upper view of the rear-end impact beam
Source: Authorship using simulation software.

OBJECTIVE

By exposing the severity of body intrusion in collisions involving seven-seater vehicles, this project has the goal of increasing the safety of third row occupants by reducing body intrusion in these types of collisions.

METHODOLOGY

Explicit dynamic computational simulation models were developed to evaluate the performance of the solution proposed in this article. The models were created considering the limitations imposed by the student license of the simulation software used, most notably the 128,000-element cap for each model's mesh.

Initially, a CAD model of a vehicle body was designed to serve as a generic representation with sufficient similarity to most seven-seater SUVs that make up the Brazilian vehicle fleet.

The body-in-white model used for the study was based on two publicly available CAD models, which were adapted to generate a geometry better suited to the objectives of this project, thereby overcoming the challenge of accessing and publishing the detailed structural model of a currently marketed vehicle.

The two CAD models used as references are shown in Figures 7 and 8. Figure 9 presents the CAD model developed by the research group for this study

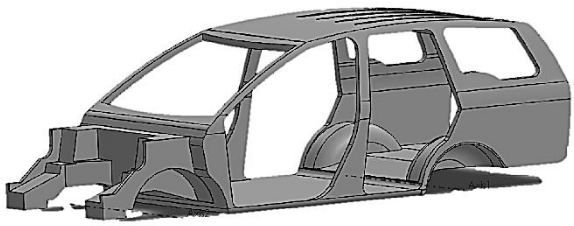

Figure 7: Simplified CAD of the body of a Mahindra XUV 500
Source: Yahya Ansari [4]

Figure 8: Simplified generic chassis
Source: Nabin Mishra [5]

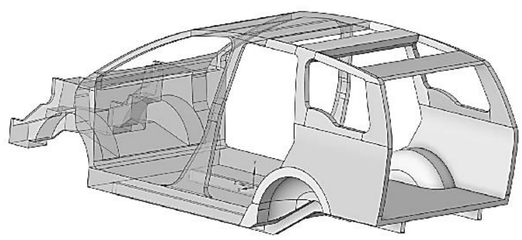

Figure 9: CAD authored by itself to carry out the simulation
Source: Authorship using simulation software.

The study was conducted to compare the performance of the developed model before and after the implementation of the proposed solution, under different impact conditions defined according to the requirements of the international vehicle crash standards previously mentioned.

The main objective of the computational analysis was to evaluate the variation in intrusion within the developed model, comparing results before and after the solution's implementation, followed by an assessment of the model's overall behavior and the performance of components of interest in terms of energy absorption.

An initial simulation model was developed and yielded promising results. However, when tested under higher-speed collision scenarios, its behavior was deemed unrepresentative of real-world conditions. Consequently, a second model was configured, which demonstrated a behavior considered to be more consistent with actual severe crash scenarios.

The meshes used for each model were developed with the aim of achieving the highest possible consistency between them. It is worth noting that they were also designed to strike an optimal balance between the limitations of the software license, result accuracy, and computational power requirements.

Shell-type elements were used, ensuring that they were predominantly quadrilateral and with minimal size variation across the mesh. For the discretization of the impact absorption assembly added to the vehicle body, a thinner mesh was required in comparison to the rest of the model to properly capture the stress concentration at the impact bar supports.

The initial conditions for each model were defined based on international vehicle crash standards, as previously mentioned. In both models, the vehicle is initially at rest with its translation constrained to prevent part of the impact barrier's kinetic energy from being transferred to the vehicle body as rigid-body motion. This ensures that the entire energy transfer occurs through deformation mechanisms.

The impact barrier moves toward the vehicle with an initial velocity of 38 km/h and 80 km/h for the first and second cases, respectively. The mass of the barrier also differs between the two cases: 1,100 kg for the first and 1,361 kg for the second.

However, there are differences in how the vehicle is represented in each scenario. In the first case, only the rear portion of the vehicle body was modeled, as it was the designated region of interest for the project. The total number of elements in this model was 66,180. In the second case, the full vehicle body was represented. This change was made after it was observed that additional structural regions contributed to the model's behavior during development. The aim was also to achieve a more comprehensive representation of the system. Consequently, the second simulation included 104,480 elements. Figures 10 and 11 show the different generated meshes.

Finally, both the impact barrier and those regions of the vehicle body not considered the focus of this study were defined as rigid bodies. This approach helped reduce both the required computational power and the total number of elements in the mesh, while maintaining the same element size in the rear region of the body—highlighted in Figure 10 which was the primary focus of the analysis in both models. As such, performing simulations with the entire body modeled as a deformable structure is considered a future step for improving and deepening this study, contingent on the availability of greater computational resources and access to the detailed CAD model of a real vehicle selected as the object of study.

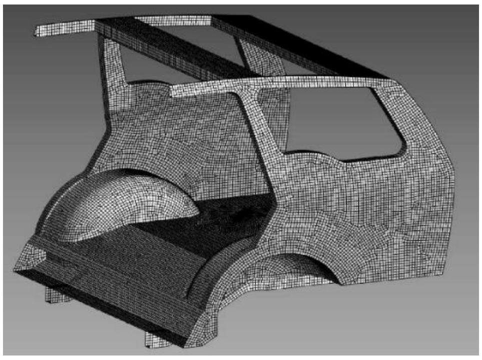

Figure 10: Mesh produced for the first simulation
Source: Authorship using simulation software.

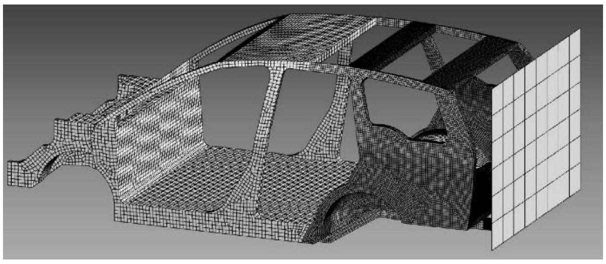

Figure 11: Mesh produced for the second simulation
Source: Authorship using simulation software.

RESULTS

For the first simulation, a maximum intrusion of 166.38 mm was observed for the model without the implementation of the proposed improvement, called the control model. In the model with the improvement implemented, the intrusion became 98.36 mm, representing an improvement of 40.89% in intrusion. Figure 12 represents the improvement obtained in the first simulation.

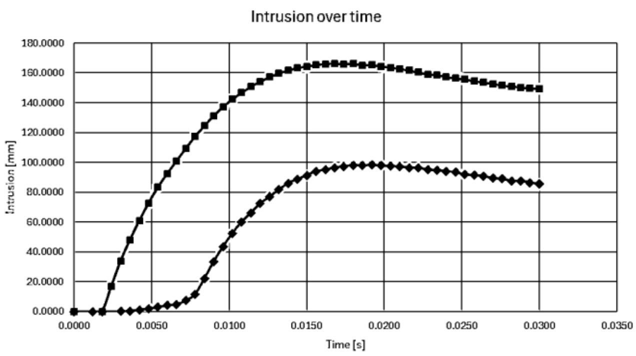

Figure 12: Body intrusion over time in the first simulation
Source: Authorship using data from simulation software.

The following figures illustrate the deformation mode observed for the control model and the model with the solution, respectively:

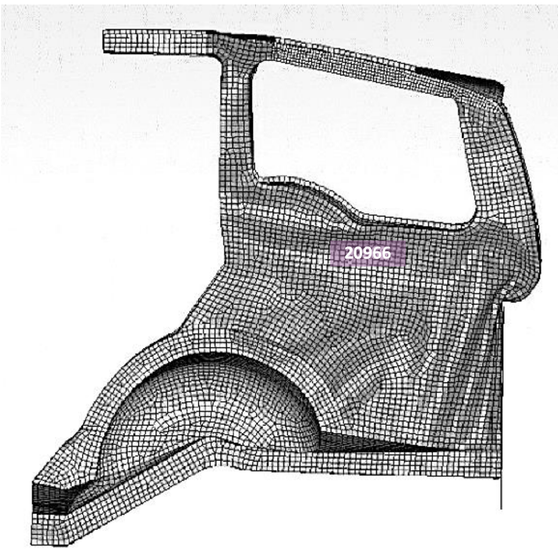

Figure 13: Deformation in the control model (first simulation)
Source: Authorship using simulation software.

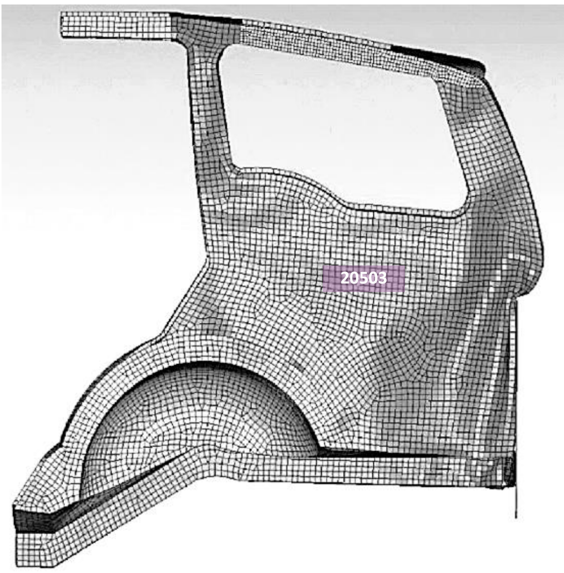

Figure 14: Deformation in the first model with the solution
Source: Authorship using simulation software.

The energy absorbed over time by the parts most relevant to the model was also investigated, as well as the sum of the energy absorbed by these parts. The graph in figure 15 shows that the crash bar supports are the parts with the highest energy absorption, followed by the side panel on each side. The graph in figure 16 shows the same study, but in relation to the total energy of the system. This set of parts was responsible for absorbing 63% of all the energy present in the collision.

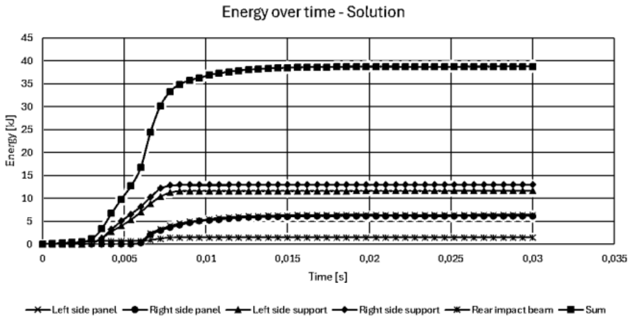

Figure 15: Graph the energy absorbed [kJ] per second with the implemented solution
Source: Authorship using data from simulation software.

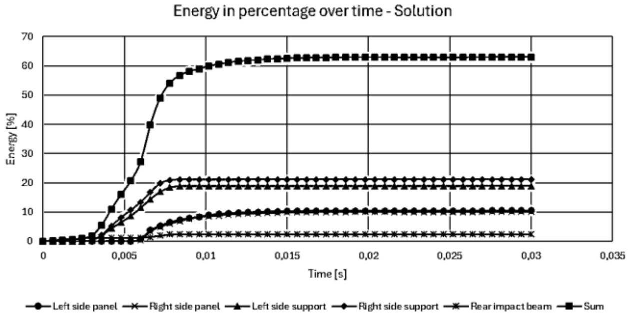

Figure 16: Graph of energy absorbed [%] per second with the solution implemented
Source: Authorship using data from simulation software.

Making the same comparison as the first simulation model, a maximum intrusion of 339.39 mm was observed for the control and 285.08 mm for the model with the proposed improvement in the second simulation. As a result, there is a 16% improvement in intrusion for the model studied with an impact at 80 km (about 49.71 mi/h).

The behavior observed for this model was considered more consistent with what is observed in high-speed accidents, but it is worth noting that it is still not considered fully representative. Figure 17 shows the improvement obtained in the simulation of the second model.

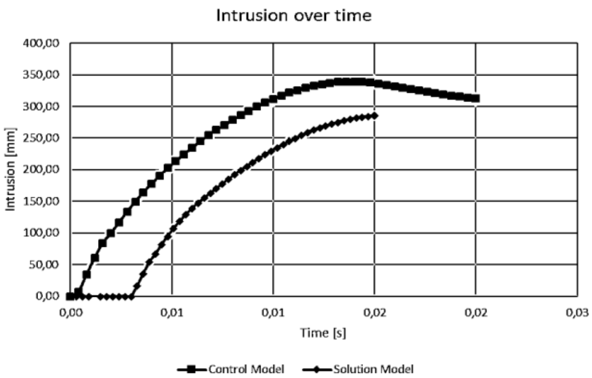

Figure 17: Body intrusion over time in the second simulation
Source: Authorship using data from simulation software.

In a similar way to what was done with the previous simulations, figures 18 and 19 represent a lateral view of the deformation before and after the application of the proposed solution, respectively:

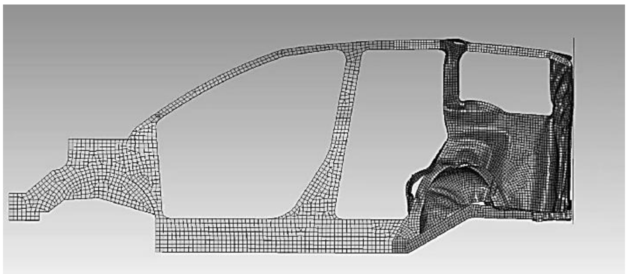

Figure 18: Deformation in the Control Model (Second Simulation)
Source: Authorship using simulation software.

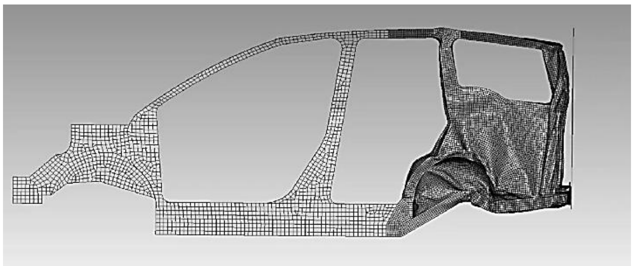

Figure 19: Deformation in the second model with the solution
Source: Authorship using simulation software.

Figure 20 shows the deformation suffered by the rear end impact beam support at 4 different time instants. It should be noted that the deformation suffered by these parts begins in the region of the restriction, made to introduce a programmed deformation zone in this part.

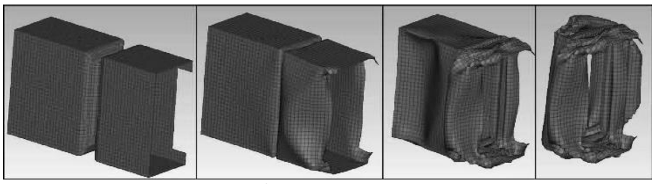

Figure 20: Deformation in the beam support
Source: Authorship using simulation software.

On the other hand, the impact bar exhibits no significant plastic deformation. Instead, plastic deformation is observed only in the areas where it contacts the supports, as highlighted in Figure 21. One possible cause for this behavior is the absence of programmed crumple zones, such as those present in the substrates.

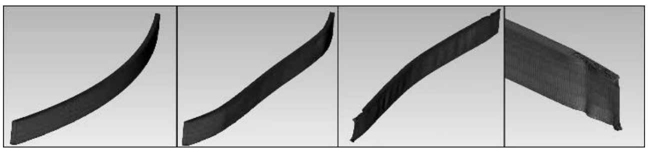

Figure 21: Deformation of the impact attenuator plate bar
Source: Authorship using simulation software.

When analyzing the distribution of energy absorbed by each component of the added impact absorption system, it is evident that the supports absorb significantly more energy than the impact bar. This behavior is attributed to the low plastic deformation experienced by the bar, due to the lack of programmed deformation zones, which in future studies may be linked to its geometric design.

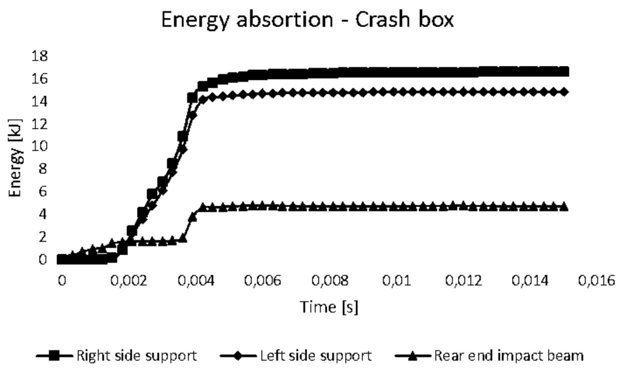

Figure 22: Energy absorbed in the region of Crash box
Source: Authorship using data from simulation software.

For the control model, it was observed that the five components or sets of components with the highest energy absorption accounted for 93% of the total energy absorbed by the vehicle during impact, with the vehicle floor alone absorbing 66% of this energy. In the improved model, it is noteworthy that the energy absorbed by the floor decreased, now representing 46% of the total energy absorbed by the vehicle.

This can be explained by better energy distribution resulting from the proposed improvements, as evidenced by the subsequent sets of components that absorb the most energy, three of which are directly addressed by the enhancement. In the improved model, the five indicated components account for 89% of the system's total absorbed energy. These data are illustrated in Figures 23 and 24 below.

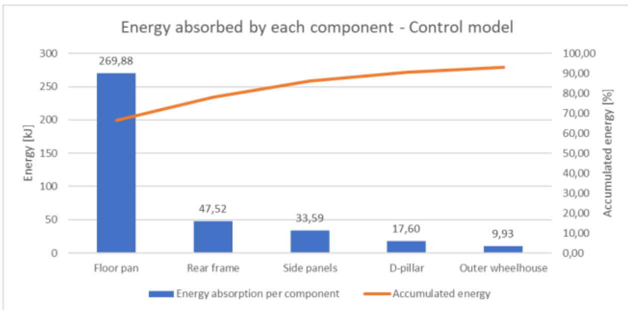

Figure 23: Energy absorption per part in control model
Source: Authorship using data from simulation software.

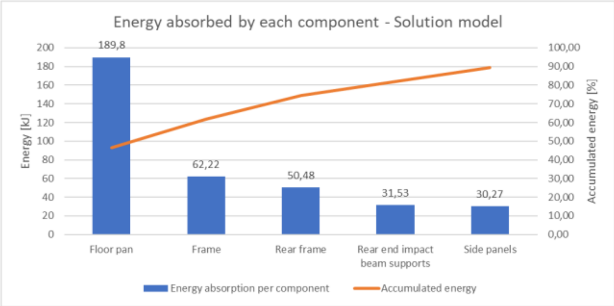

Figure 24: Energy absorption per part in the improved model
Source: Authorship using data from simulation software.

Finally, the energy absorbed by each component added or modified through the proposed improvement was evaluated. Figure 25 demonstrates the minimal contribution of the rear D-crossmember and the lateral closing crossmembers. It is evident that these components account for a very small portion of the total energy absorption, thereby contributing little to the project's primary objective.

The low performance of these components may be attributed to their geometry in the 3D model utilized, which warrants further investigation in future studies. It is also noteworthy that the performance of the impact bar could be enhanced through the incorporation of programmed crumple zones, as previously mentioned.

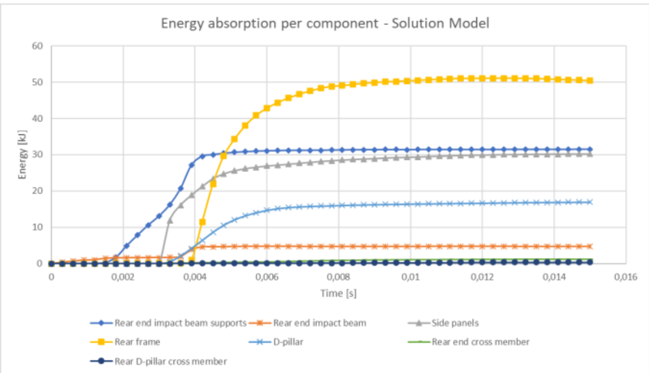

Figure 25: Energy absorbed per solution part set
Source: Authorship using data from simulation software.

Figure 26 provides an overview of the proportion of energy absorbed by all components directly affected by the proposed improvement. It is observed that the improvement itself is capable of absorbing 33% of the system's total energy. However, as noted earlier, the proposed enhancement also contributed to redirecting part of the system's energy to other vehicle body components, such as the stringers.

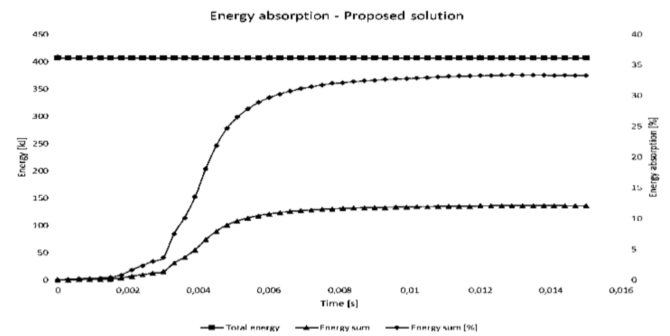

Figure 26: Total energy absorbed in the proposed improvement
Source: Authorship using data from simulation software.

CONCLUSION

The reduction in intrusion in rear end collisions was significant when the solution was applied. This reduction is due to the introduction of steel with greater energy absorption at the rear of the vehicle, which helps to direct the energy to other areas of the body. In addition, the implementation of the rear end impact beam contributes positively to the reduction of intrusion, being an additional piece to the vehicle's current structure to mitigate the impact energy to be absorbed by the body.

With the simulations carried out, the reduction in intrusion reached 40.89% at low speeds. At high speeds, the reduction in intrusion was 16%. This difference from the target is due to the limited simulation conditions and the high impact energy involved (collision causing object with more mass and more speed compared to the first simulation).

The objective of the project is therefore achieved, as it's possible to observe a reduction in body intrusion in seven-seater vehicles in the event of a rear-end collision.

REFERENCES

[1] BRAZIL. Anuário 2022, from May 8th, 2023. Polícia Rodoviária Federal. Brasília, Brazil. Available at: https://www.gov.br/prf/pt-br/acesso-a-informacao/dados-abertos/diest-arquivos/anuario-2022_final.html. Access on April 19th, 2024.

[2] DIRMAVE. Consulta de Veículos. Distribuidora Riomafrense de Veículos S.A. Available at: www.dirmave.com.br. Access on October 18th, 2023.

[3] BRAZIL. Resolution n. 721, from January 10th, 2018. Diário Oficial da União, Ministério da Infraestrutura/Conselho Nacional de Trânsito, Brasília, Brazil. January 10th, 2018. Available at: https://www.gov.br/transportes/pt-br/assuntos/transito/conteudo-

contran/resolucoes/resolucao7212018.pdf. Access on December 10th, 2023.

[4] ANSARI, Yahya. XUV 500 (for project). Available at: https://www.grabcad.com/library/xuv-500-for-project-1. Access on April 19th, 2024

[5] MISHRA, Nabin. Car chassis. Available at: https://www.grabcad.com/library/car-chassis-13. Acess on: April 19th, 2024.